THERMAL MODELLING OF THE CUTTING PROCESS USING FEM SIMULATION WITH UPDATED THERMOPHYSICAL PROPERTIES OF TOOL MATERIALS

Piotr Niesłony

Summary

This study compares two variants of the FEM simulation model of orthogonal cutting process of C45 carbon steel with multilayer-coated tools. In particular, new data on the thermophysical properties of the substrate and coating materials, measured by means of the advanced Laser Flash and Differential Scanning Calorimeter methods, were applied. Both simulation algorithms use the Power Law constitutive model, similar to the Johnson-Cook law but the second variant, termed Power Law–Temperature Dependent (PL-TD) algorithm, takes into account the temperature-dependent thermophysical properties of the tool. In this study, the temperature distribution, heat flux intensity and tool-chip contact length were validated based on the appropriate measurements.

Keywords: thermal behaviour, FEM simulation, coated tools.

Modelowanie cieplnych oddziaływań w procesie skrawania z zastosowaniem symulacji MES i cieplnofizycznych właściwości materiału narzędzia

Streszczenia

W artykule porównano dwa warianty symulacyjne modelu MES procesu ortogonalnego skrawania stali węglowej C45 narzędziem z powłoką wielowarstwową. Wprowadzono nowe dane cieplnofizycznych właściwości materiału substratu i powłoki określone zaawansowanymi metodami różnicowej kalorymetrii skaningowej oraz Laser-Flash. Oba zastosowane algorytmy symulacji wykorzystują wykładniczy model konstytutywny, zbliżony do modelu Johnsona-Cooka. Drugi wariant, określany Power Law-Temperature Dependent (PL-TD), uwzględnia zależne od temperatury właściwości cieplnofizyczne materiału narzędzia. W prowadzonych badaniach rozkład temperatury, intensywność strumieni ciepła oraz długość kontaktu wiór-ostrze zweryfikowano w oparciu o uzyskane wyniki pomiarowe.

Słowa kluczowe: oddziaływania cieplne, symulacje MES, narzędzia z powłoką wielowarstwową

1. Introduction

In order to implement a range of advanced machining technologies, including especially high-speed and dry or near dry processes, modern machine

Address: Piotr NIESŁONY, D.Sc., Eng., Department of Manufacturing Engineering and Production Automation, Opole University of Technology, 45-271 Opole, 5th Mikolajczyka St., Poland, p.nieslony@po.opole.pl

shops employ cutting tools treated with more sophisticated coatings [1]. Roughly speaking, today more than 80% of all machining operations are performed with cutting tools coated mainly with titanium and aluminum based, differently-structured thin films. Moreover, the trend towards more economical and less costly processes leads to wider testing of the machining operations by means of engineering simulation tools, among which the Finite Element Method (FEM) seems to play the predominant role. Unfortunately, until now a few FEM-based simulation techniques (Lagrangian, Eulerian, ALE) used are not able to model integrally all physical phenomena involved into complex machining process (chip formation, plastic deformation, cutting forces, heat transfer, tool wear as well as surface finish and state of the subsurface layer) with engineering accepted accuracy [2]. According to specialists in metal-cutting simulation area, the barriers in developing more effective FEM algorithms are insufficient mechanical and thermo-physical data on both workpiece and cutting tool materials. For example, apart from many professional FEM packages available, the accuracy of simulation suffers from improper material constitutive laws and material thermal properties, including coating components and integrally substrate-coating systems. The thermal or thermodynamicall modelling is a bottleneck of FEM simulation due to uncertainties in arbitrary using such inputs as heat partition coefficient, friction coefficient and both thermal conductivity and diffusivity. Some successful initiatives regarding multilayer coatings were previously undertaken by Grzesik [3, 4], Attia et al. [5], Davies et al. [6], Rech et al. [7], Özel [8] and more recently by Ceretti et al. [9] and Pujana et al. [10]. They deal with including such specific aspects as: thermal-dependent physical properties [3], composite layer concept [4], thermal constriction resistance phenomenon [5], uncertainties in material data and its effect on the discrepancies between modelled and IR-measured temperature [6], heat transfer in various domains of time [7], tool-chip interfacial friction models [8], the global heat transfer coefficient in ALE formulation [9] and the inverse identification algorithm for flow stress data [10]. In this paper, the updated thermal properties of WC-6%Co substrate and multilayer CVD-TiC/Al_2O_3/TiN coating system, recently determined by means of the advanced Laser Flash and Differential Scanning Calorimeter methods in the Netzsch' research centre, Germany, were implemented into the Lagrangian-FEM model.

2. Experimental Program

2.1. Determination of thermophysical properties of cutting tool materials

A scheme of laser flash (LF) apparatus is shown in Fig. 1. The sample is mounted on a carrier system which is located in a furnace during the measurements. After the sample reaches a pre-determined temperature, a burst

of energy emanating from a pulsed laser is absorbed on the front face of the sample, resulting in homogeneous heating.

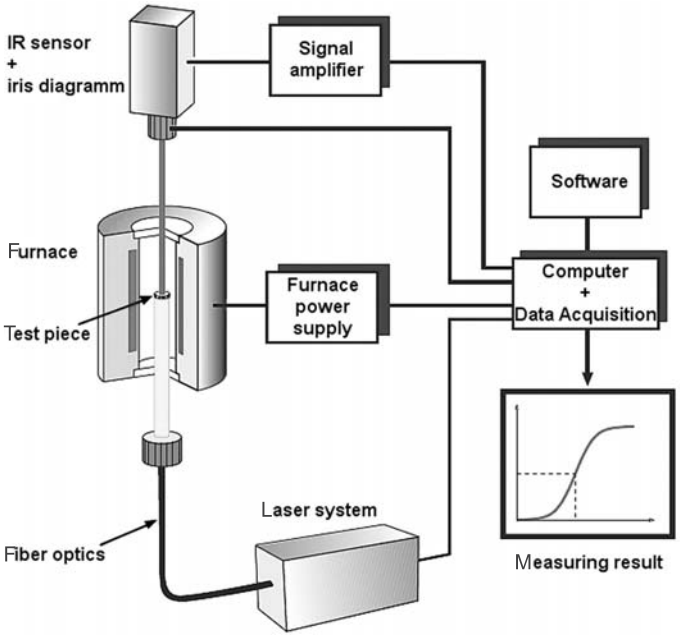

Fig. 1. Laser flash apparatus for determining thermal diffusivity [11]

The relative temperature increase on the rear face of the sample is then measured as a function of time by an IR detector. First, the thermal diffusivity is computed by software using the time relative temperature increase data. For adiabatic conditions, α is determined from the simple equation:

$$\alpha = 0.1388 l^2 / t_{0.5} \tag{1}$$

where: l is the sample thickness in mm and $t_{0.5}$ is time (in sec) at 50% of the temperature increase.

On the other hand, the temperature-dependent thermal conductivity $\lambda(T)$ was determined by prior measuring the thermal diffusivity (α), the specific heat (c_p) by means of a differential scanning calorimeter (DSC), and density (ρ), all as functions of temperature. That is:

$$\lambda(T) = \alpha(T)\rho(T)c_p(T) \tag{2}$$

2.2. Inputs data to the FEM simulation package

In this study, an updated Lagrangian finite element formulation is used to predict the thermal behaviour in orthogonal cutting of C45 medium carbon steel with CVD-TiC/Al_2O_3/TiN coated tools. Both standard and PL-TD material models available in the FEM software AdvantEdge [12] were used. The PL-TD approach uses also the standard Power Law constitutive model but the user can vary thermal conductivity and heat capacity as functions of temperature (Eqns. 3-5).

$$\lambda = 73.154 + 3.71895 \cdot 10^{-3} \cdot t - 1.6081 \cdot 10^{-5} t^2, \text{ W/m} \cdot \text{K} \tag{3}$$

$$\alpha = 2.12483 \cdot 10^{-5} - 9.0932 \cdot 10^{-9} \cdot t + 8.2217 \cdot 10^{-13} t^2, \text{ m}^2/\text{s} \tag{4}$$

$$c_p = 237.429 + 0.16352 \cdot t - 6.1164 \cdot 10^{-5} t^2, \text{ J/kg} \cdot \text{K} \tag{5}$$

In addition, three layer coating was replaced by a homogeneous layer with equivalent thermal properties (curve 3L in Fig. 2) described in Refs. [4, 13]. Moreover, the second option was examined by providing the values of thermal properties of the substrate-coating system (3L-N curve in Fig. 2) measured by means of the LF and DSC apparatus (see Section 2.1).

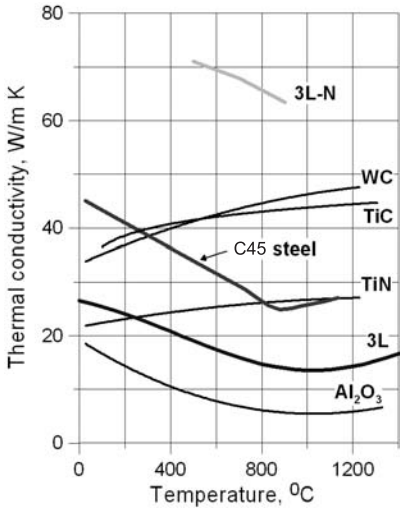

Fig. 2. Thermal conductivity of tool (substrate, coatings) and workpiece materials vs. temperature

Another inputs were values of the friction coefficient (0.631, 0.577 and 0.508 for P20 carbide tools and 0.676, 0.605 and 0.515 for 3L-coated tools) obtained experimentally for the three cutting speeds selected (103.2, 206.4 and 330 m/min) and feed rate of 0.16 mm/rev. It tends to be close to 0.5 at v_c = = 330 m/min. The average density of the cutting tool material (substrate plus coating) was assumed to be equal to 1379.4 kg/m^3.

3. Experimental results and discussion

3.1. Cutting temperature

Comparison of the predicted and measured values of the average tool-chip temperature for uncoated and coated tools and three selected cutting speeds are shown in Fig. 3. In general, the "standard" simulation provides substantially

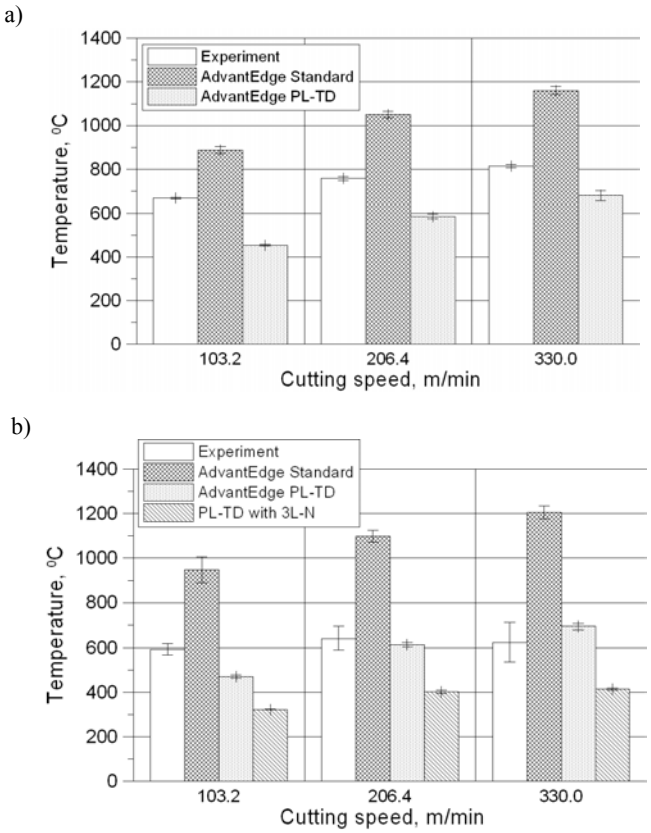

Fig. 3. Comparison of the measured cutting temperature with FEM simulated values. Tool material: a) ISO P20 carbide, b) 3L coating. Confidence interval P = 95%

higher temperature in comparison with thermocouple-based measurements. Better agreement was achieved in the PL-TD option and in case of coated tools for higher speeds, i.e. 200-330 m/min. On the other hand, for the Netzsch's data the predicted temperature underestimate distinctly the measurements (differences are even higher than 50%). This discrepancy suggests that microscopic approach to the substrate-coating system does not improve the simulation efficiency and assuming the composite layer approach with equivalent thermal properties seems to be more appropriate.

3.2. Distribution of temperature within the tool body

The temperature along the tool-chip interface and beneath the rake face in the point of peak temperature (at a distance of 0.18 mm from the cutting edge) predicted for different simulation conditions, are shown in Figs. 4a and 4b respectively. It is evident from Fig. 4a that the standard FEM simulation

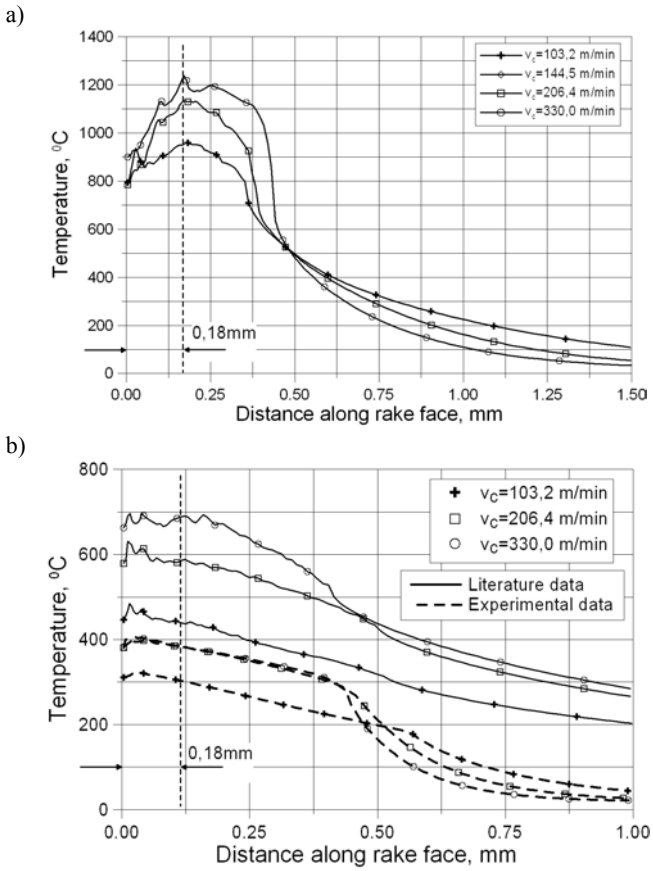

Fig. 4. Temperature distribution along rake face vs. cutting speed for C45 carbon steel and 3L coated tools: a) standard FEM, b) PL-TD

generates temperature distribution curves with distinct peaks, which are localized at a constant distance of 0.18 mm from the cutting edge. For the PL-TD option a small plateau in the 0.18 mm wide area is a characteristic feature of these distributions (Fig. 4b). It should also be noticed that shorter distance from the cutting edge to the point with temperature stabilization were observed for coated tools. The reduced von Mises stress distribution along the tool-chip interface for different simulation conditions is shown in Fig. 5. The zone Ia of can be referred to the seizure region with intensive adhesive interaction. In addition, the boundary between the first (I) and second (II) zones coincides with the points of maximum interface temperature.

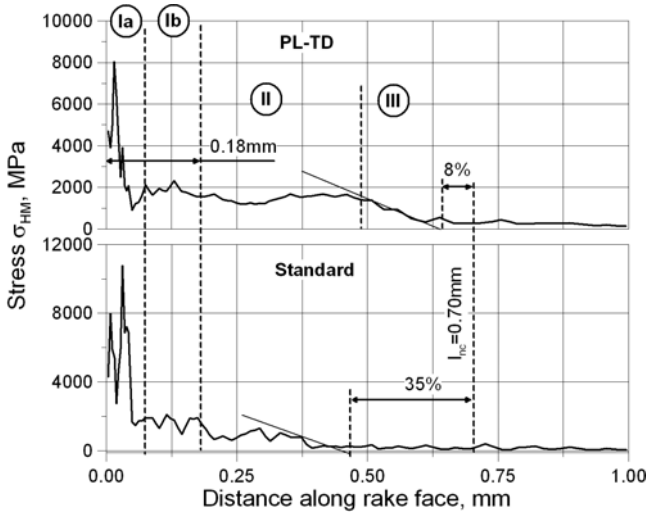

Fig. 5. Distribution of the reduced von Mises stress along rake face for C45 carbon steel and 3L coated tools (v_c = 206.4 m/min)

The influence of the three layer coating on the temperature distribution beneath the tool-chip interface can be assessed based on the confrontation of the relevant distribution curves shown in Figs. 6 and 7. For uncoated tools, temperature decrease monotonically and the temperature gradients vary between 470-720°C/mm. They are practically the same regardless of the simulation option employed. In contrast (Fig. 7), for coated tools and the cutting speed of 330 m/min, this gradient reaches about 3000°C/mm (equivalently 3.0°C/μm) which documents well the thermal barrier effect caused by the Al_2O_3 ceramic interlayer. In summary, the heat penetration effect is four times less than for uncoated carbide tools applied.

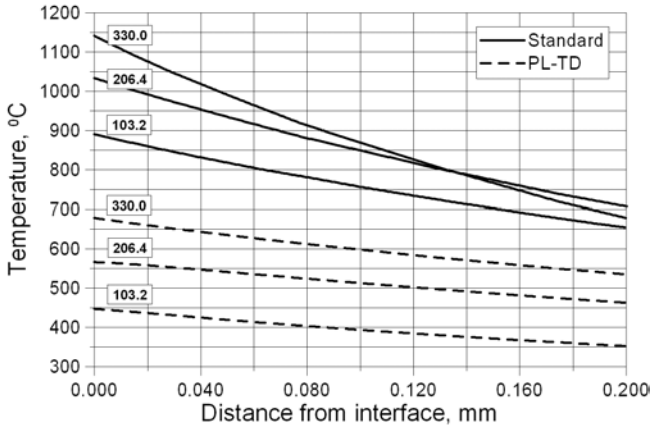

Fig. 6. Temperature distribution below the rake face in the point of maximum contact temperature for C45 steel and P20 carbide tools

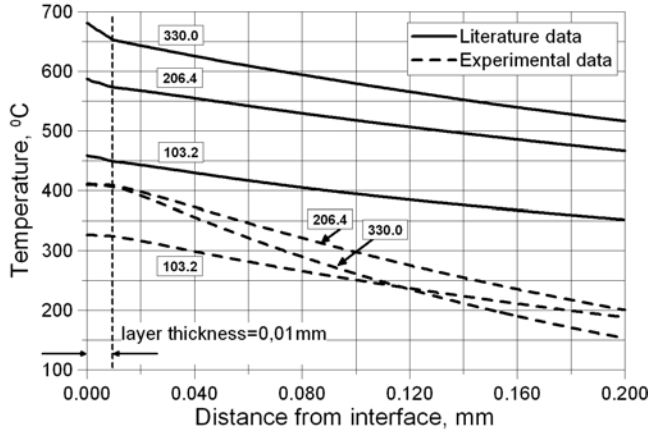

Fig. 7. Temperature distribution below the rake face in the point of maximum contact temperature for AISI 1045 steel and 3L coated tools (PL-TD option)

3.3. Visualization of thermal behaviour of the cutting zone

Some characteristic temperature maps covering the primary (PDZ) and secondary (SDZ) deformation areas obtained for different thermophysical data are shown in Fig. 8. In case of the PL-TD variant (Fig. 8b) the chip is visibly thicker and the field of higher temperatures is more extended in the chip. On the other hand, the maximum temperature of about 700°C is localized closer to the cutting edge and the tool contact area is cooler (about 550°C). For example, the

relevant temperature recorded for "standard" simulation (Fig. 8a) is equal to 1020°C and 950°C, respectively.

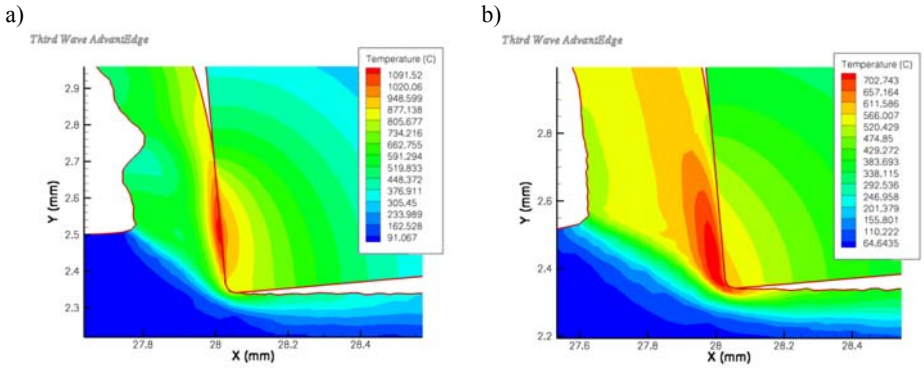

Fig. 8. Thermal maps for C45 carbon steel and 3L coated tools obtained by: a) standard FEM, b) PL-TD option (v_c = 206.4 m/min)

In order to compare intensities of heat fluxes in the SDZ, the special statistical procedure, which divides the sorted data set into some parts, was applied. It includes median, lower 2 (cuts off lowest 25% of data) and upper 1 (cuts off highest 25% data) quartiles and their maximum values 3 recorded. The relevant graphs obtained are shown in Fig. 9.

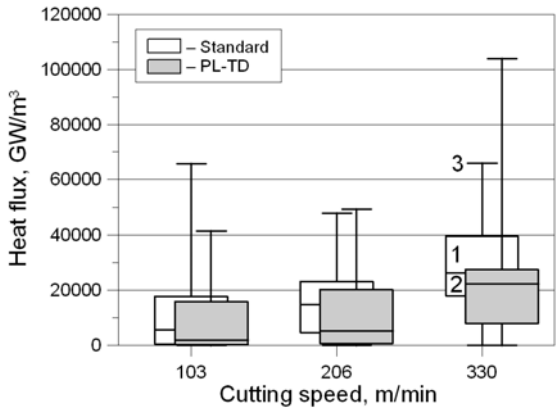

Fig. 9. Heat flux vs. cutting speed for 3L-coated tools showing median, lower and upper quartiles and maximum values

Generally, the frictional component of heat flux for both simulation algorithms increases slowly with the increase of the cutting speed. In case of coated tool, more heat produced by friction has been recorded for standard FEM

simulation. Also the differences with temperature predicted for standard and PL-TD approaches can be explained in terms of visible differences in the magnitudes of heat fluxes illustrated in Fig. 9. The differences of the peak temperatures for the same cutting speed of 206 m/min but for various simulation options (1100^{o}C vs. 615^{o}C in Fig. 3b) can be explained in terms of the displacement of the lower quartile, in case of the standard simulation, up to 5000 GW/m^3. For the PL-TD method the lower quartile starts to fluctuate from approximately zero. In general, the trend showing the increase of the contact temperature with cutting speed is documented by localization of the median (horizontal line within the flux box).

4. Summary

- Simulation option and input thermophysical data of the tool materials are decisive factors in obtaining proper temperature values in both PDZ and SDZ.
- For 3L coated tools the best coincidence of experimental and modelled temperature were obtained for PL-TD option and composite coating which represents "micro" approach to thermal functions of the coating deposited.
- Temperature distribution patterns have some visible physical analogies to the reduced von Mises stresses and tool-chip contact behaviour.
- The differences in thermal behaviours of uncoated and coated tools, especially those related to the intensity and fluctuation of the heat fluxes in the seizure region, can be clarified in terms of quartiles. In general, the trend showing the increase of the contact temperature with cutting speed is documented by different localization of the median.

Acknowledgements

This research is supported by the Ministry of Science and Higher Education under Grant no. N503 026 31/3171, in 2006-2008.

References

[1] F. KLOCKE, T. KRIEG: Coated tools for metal cutting-features and applications. *Annals of the CIRP*, **48**(1999)2, 515-525.
[2] T.H.C. CHILDS, K. MAEKAWA, et al.: Metal cutting. Theory and applications. Arnold, London 2000.
[3] W. GRZESIK: An Investigation of the thermal effects in orthogonal cutting associated with multilayer coatings. *Annals of the CIRP*, **50**(2001)1, 53-56.
[4] W. GRZESIK: Analytical models based on composite layer for computation of tool-chip interface temperature in machining steels with multilayer coated cutting tools. *Annals of the CIRP*, **54**(2005)1, 91-94.

[5] M.H. ATTIA, L. KOPS: A new approach to cutting temperature prediction considering the thermal constriction phenomenon in multi-layer coated tools. *Annals of the CIRP*, **53**(2004)1, 47-52.
[6] M.A. DAVIES, Q. CAO, A.L. COOKE, et al.: On the measurement and prediction of temperature fields in machining AISI 1045 Steel. *Annals of the CIRP*, **52**(2003)1, 77-80.
[7] J. RECH, J.L. BATTAGLIA, A. MOISAN: Thermal influence of cutting tool coatings. *J. Mat. Proc. Technol.*, **159**(2005), 119-124.
[8] T. ÖZEL: The influence of friction models on finite element simulation of machining. *J. Mach. Tools Manuf.,* **46**(2006), 518-530.
[9] E. CERETTI, L. FILICE, D. UMBRELLO, et al.: ALE simulation of orthogonal cutting: a new approach to model heat transfer phenomenon at the tool-chip interface. *Annals of the CIRP*, **56**(2007)1, 69-72.
[10] J. PUJANA, P.J. ARRAZOLA, R.M. M'SAOUBI, et al.: Analysis of the inverse identification of constitutive equations applied in orthogonal cutting process. *J. Mach. Tools Manuf.,* **47**(2007), 2153-2161.
[11] Laser Flash Apparatus LFA 427, www.Netzsch.com.
[12] Third Wave *AdvantEdge* 2D User's Manual, Version 5.0, 2006, Minneapolis, USA.
[13] W. GRZESIK, M. BARTOSZUK, P. NIESLONY: Finite element modelling of temperature distribution in the cutting zone in turning process with differently coated tools. *J. Mat. Proc. Technol.,* **164-165**(2005), 1204-1211.

Received in May 2008